Simulation of Human MicroDopplers Using Computer Animation Data

Shobha Sundar Ram and Hao Ling, *Fellow*, IEEE
Dept. of Electrical and Computer Engineering, University of Texas at Austin
1 University Station, 78712, Austin, Texas, USA
phone: +(1) 5124711910, fax: +(1) 5124711910, shobhasram@mail.utexas.edu, ling@ece.utexas.edu

***Abstract*—The capability to detect, track and monitor human activities in non-line-of-sight environments is an important component of security and surveillance operations. The movement of the human body and limbs result in unique microDoppler features which can be exploited for identification and classification of different types of human motions. In this paper, a method to simulate the microDoppler signatures of complex human motions from virtual reality animation data is presented. The simulation method is tested on three types of human motions - walking, running and crawling. The simulated Doppler spectrograms are compared with measurement results. Additional simulation data are presented to show patterns over a long time duration and the effect of frequency and viewing angle.**

***Index Terms*—Doppler spectrogram, microDoppler, human activities, computer animation data, radar cross-section**

I. Introduction

Detection and monitoring of human activities have important applications in security and surveillance operations. For this purpose, different types of sensors have been developed such as optical, infrared and RF sensors. One of the unique advantages offered by an RF sensor system is the capabilities of operating in non-line-of-sight situations such as through building walls and over 24-hour, all-weather conditions. Doppler-based RF sensors, in particular, are useful for detecting human motions since stationary clutters from the background environment are suppressed. Furthermore, low-cost commercial sensor components are readily available at microwave frequencies.

Human Doppler returns are characterized by unique microDoppler features that result from the dynamic movements of the different body parts [1-3]. The microDoppler features are best observed using joint time-frequency representations such as the short-time Fourier transform (STFT) [1, 2]. The resulting Doppler spectrograms can be used for identifying and classifying different types of motions [4, 5]. In addition to measurement data collection, it is useful to develop the capability to simulate such microDoppler data from different human movements. Such a tool can provide the means to pinpoint cause-and-effect for phenomenology interpretation and to generate training data for algorithm development. To date, models have been developed to simulate the constant velocity walking motion of a human [1, 3]. In [1], infrared motion capture data of the different limbs were combined with a point scatterer model to generate the Doppler spectrogram. In [3], the Thalmann model for human gait was used in conjunction with a primitive based predictor to generate the Doppler spectrogram. However, Doppler signatures have not been simulated for more complex human motions.

In this paper, we generate radar microDoppler data of human motions using the computer animation data that are available from the video gaming and animation movie industries. Different formats of animation data files are available. Here we use BioVision's BVH data format and Acclaim's ASF/AMC data format to simulate different human motions. The simulation results are verified by conducting measurements on a human subject with a Doppler radar testbed in the laboratory.

This work is supported by the National Science Foundation under grant CBET-0730924 and in part by a grant from the NSF Major Research Instrumentation Program.

1-4244-1539-X/08/$25.00 ©2008 IEEE

II. Simulation of Radar Returns Using Computer Animation Data

In this section, we present the methodology used to simulate Doppler radar returns using computer animation data. In the first step, we obtain the three-dimensional position of each bone of the human body at each time instant from existing animation files. In the next step, we compute the time-domain returns of the human mover by computing the radar cross section (RCS) of the human at each time instant using a primitive based predictor.

Most animation files have two parts. The first part specifies the initial pose of the human. This section is under the header 'skeleton' in the BVH data files and is a separate file with the file extension '.asf' in the ASF/AMC data format. A hierarchical distribution of the bones in the human body is described in this part. Each bone is connected to a parent bone through a joint. Bones that are not connected to child bones are terminated with end-effectors instead of joints. The relative length and orientation of each bone are specified by the vector defined between the three-dimensional positions of the two joints (or end-effector) connected to them. The center of gravity of the human lies at the root joint. The root joint is subject to 6 degrees of freedom (DOF) with respect to the initial pose. This includes translation of the position vector of the root along the X, Y and Z axes as well as Euler rotation angles (α, β, γ) about the X, Y and Z axes respectively. All the other joints are subject to 3 DOF which are the Euler rotation angles. The changes in the DOF data of the joints over time give rise to animation motion of the human. These changes are specified for each frame of the animation under the header 'motion' in BVH data files and in a separate file with the file extension '.amc' in the ASF/AMC data files.

The global three-dimensional position vector of each bone is derived using the matrix operations discussed in [6]. First, a local transformation matrix (M_{bone}) is created for each bone

Authorized licensed use limited to: Indraprastha Institute of Information Technology. Downloaded on July 20,2021 at 20:40:47 UTC from IEEE Xplore. Restrictions apply.

from the local translation (T) and rotation information of that bone. For any bone, the translation information is the offset of the bone from its parent which is specified in the skeleton section. For the root joint, the translation data is obtained from the motion section of the data file. Based on the DOF data specified for each joint by the motion section, a rotation matrix (R) is computed by multiplying 3 separate rotation matrices (R_x, R_y, R_z), one for each axis of rotation:

$$R = R_x R_y R_z \quad (1)$$

The order of multiplication of the three rotation matrices R_x, R_y and R_z is specified in the data files. The position of each bone is obtained from the transformation matrix (M) computed by concatenating the local transformation matrix of the bone with the local transformation of its parent, then its grandparent, and so on:

$$M = M_{bone} M_{parent} M_{grandparent} \cdots \quad (2)$$

In order to compute the RCS of the human, we use a primitive based model. Each body part associated with a bone is modeled as an ellipsoid. If the calibration units for the data are not specified, we scale the size of the body part to the average dimensions (height H_e and radius R_e) mentioned in [3]. The high-frequency RCS (σ) of the ellipsoid is given in [7]. Based on this approximation, the complex scattering strength of the ellipsoid can be computed using:

$$\sqrt{\sigma} = \left[\frac{\frac{1}{4}\pi R_e^4 H_e^2}{R_e^2 \sin^2\theta_e + \frac{1}{4} H_e^2 \cos^2\theta_e} \right]^{1/2} e^{-j\frac{2\pi}{\lambda}2r} \quad (3)$$

where θ_e is the angle of the incident wave with respect to the height axis of the ellipsoid, λ is the wavelength of the radar and r is the distance between the phase center of the ellipsoid and the radar. The RCS of the human is then computed by the complex sum of $\sqrt{\sigma}$ from each of the body parts. Since the human body is not perfectly metallic, the dielectric property of flesh is taken into account for the specified carrier frequency of the radar [8]. The RCS is used in the radar range equation to derive the time-domain radar returns, $x(t)$. Note that no shadowing or multiple interactions are accounted for in this model. Once the return signal is simulated, we compute the Doppler spectrogram, $\chi(t, f)$ of the motion from the short-time Fourier transform (STFT) of $x(t)$:

$$\chi(t, f) = \int x(t')h(t - t')e^{-j2\pi ft'} dt' \quad (4)$$

Here, $h(t)$, is the time window used for the STFT operation. It is important to note that the animation data is provided at a fixed frame rate usually ranging from 60 frames per second to 240 frames per second. The data need to be interpolated to provide sufficient Doppler bandwidth to avoid aliasing effects. This is particularly important at higher radar operating frequencies, since the Doppler bandwidth is directly proportional to the radar frequency. The interpolation is implemented by introducing spline interpolation to the rotational angle and translational position data obtained from the animation files.

III. Simulation Results for Walking, Running and Crawling

Using the techniques discussed above, we simulate the radar returns for human walking and running motions using BVH data obtained from Sony Computer Entertainment America. Similarly, human crawling motion is simulated using ASF/AMC data obtained from the CMU Graphics Lab Motion Capture Database. First, we assume the radar to be placed at the 3-D coordinate position (-5, 1, 0) m as shown in Fig. 1a. The carrier frequency is set at 2.4GHz. The animation data of all the three animation models specify the motion of 28 bones in the human body at a frame rate of 120 frames per second. This data is interpolated to obtain a sampling frequency of 500Hz. In the first case, the animated human walks towards the radar for 4s and then turns around and walks away from the radar. The time-domain radar returns are computed and the Doppler spectrogram is generated using a time window of 0.25 seconds and is shown in Fig. 1b. The strongest Doppler return is from the torso, which is positive when the mover approaches the radar and negative when the mover moves away from the radar. The motion of the feet and lower legs give rise to the highest Doppler returns. The motion shows periodicity that corresponds to the uniform stride motion of the human. The procedure is next repeated for running motion. In this case, the human subject runs around a circular path as shown in Fig. 1c. The Doppler spectrogram of this motion is shown in Fig. 1d. We observe that the Doppler return of the torso is much higher due to the increased speed of the body motion. The microDoppler spread is also much higher arising from the motions of the different limbs. In particular, it is now possible to observe both the front and the back swing of the lower legs and feet. At the 3.5s time instant, the Doppler track shows a steep change from positive to negative Dopplers. This corresponds to the position of the closest approach to the radar, as indicated in Fig. 1c. Finally the procedure is repeated for the crawling motion of the human subject as shown in Fig. 1e. The radar is assumed to be situated at the coordinate position (5, 1, 0) m. The Doppler spectrogram of the motion, (shown in Fig. 1f) shows considerable deviation from the spectrograms obtained from the walking and running motions. First, the torso Doppler is much lower (nearly zero) in this case. Also, the microDoppler arising from the legs are lowered and are now comparable with the microDoppler from the arms. From a detailed analysis of the simulated spectrogram, it is possible to infer that the microDoppler of the left / right arm is slightly ahead of he microDoppler of the right / left leg. The results indicate that the microDoppler signatures of human motions may be useful for identifying different types of motions.

Authorized licensed use limited to: Indraprastha Institute of Information Technology. Downloaded on July 20,2021 at 20:40:47 UTC from IEEE Xplore. Restrictions apply.

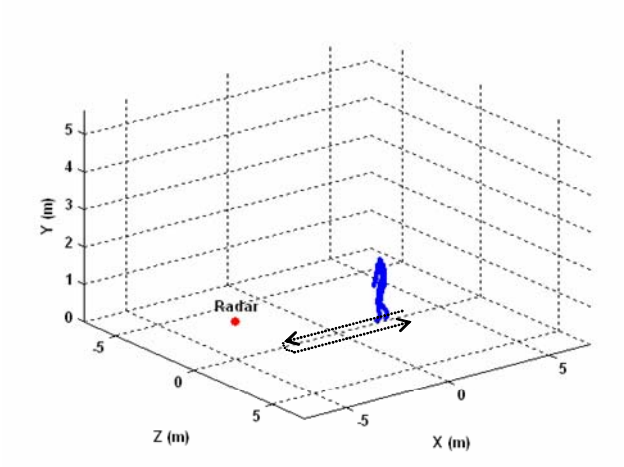

(a)

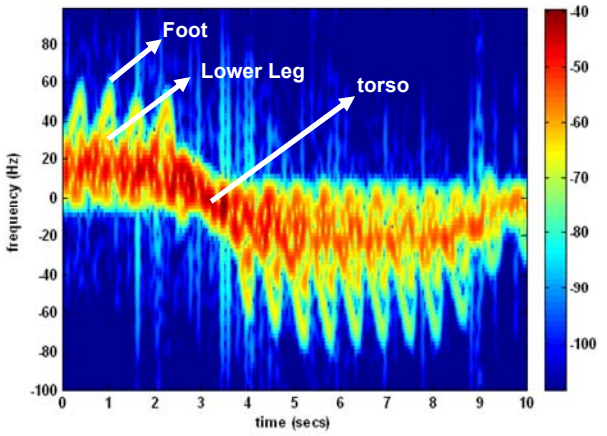

(b)

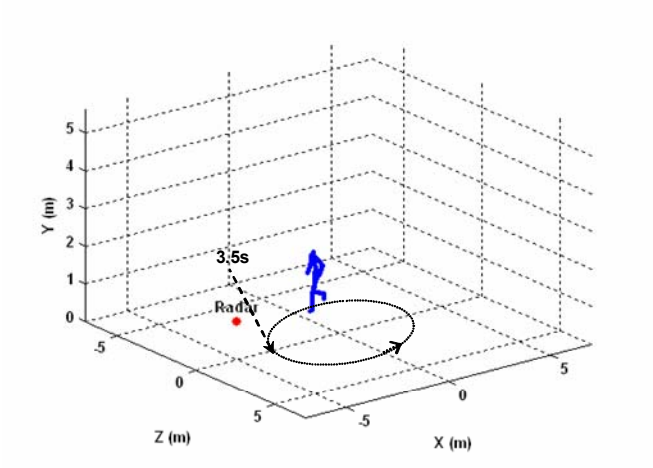

(c)

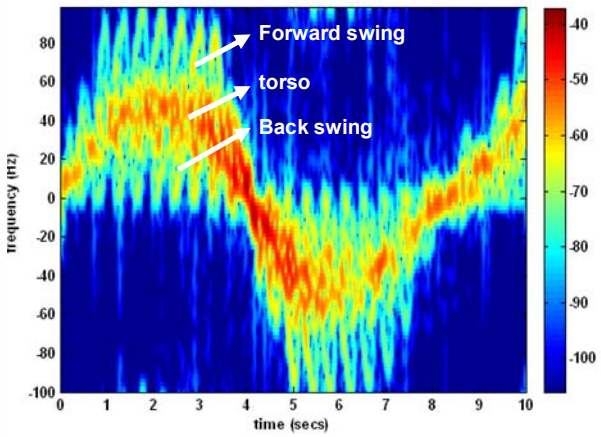

(d)

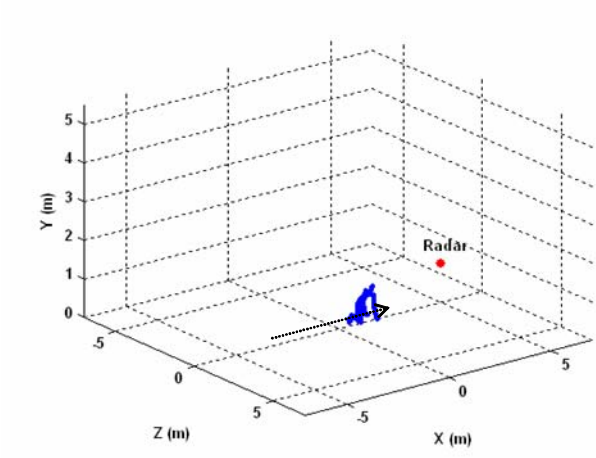

(e)

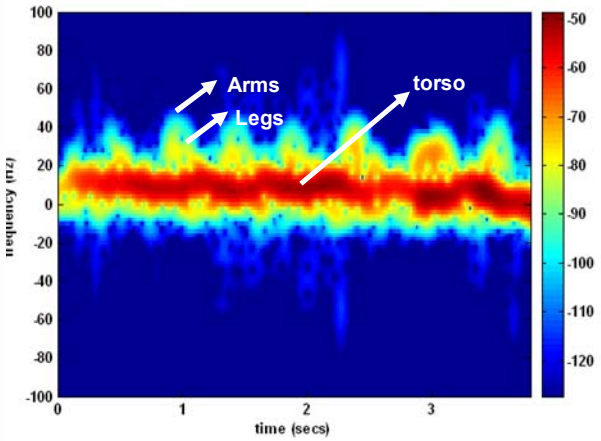

(f)

Fig.1 (a) Animation model of human walking motion, (b) Doppler spectrogram of walking motion at 2.4GHz carrier frequency, (c) Animation model of human running motion, (d) Doppler spectrogram of running motion at 2.4GHz carrier frequency, (e) Animation model of human crawling motion and (f) Doppler spectrogram of crawling motion at 2.4GHz carrier frequency.

Authorized licensed use limited to: Indraprastha Institute of Information Technology. Downloaded on July 20,2021 at 20:40:47 UTC from IEEE Xplore. Restrictions apply.

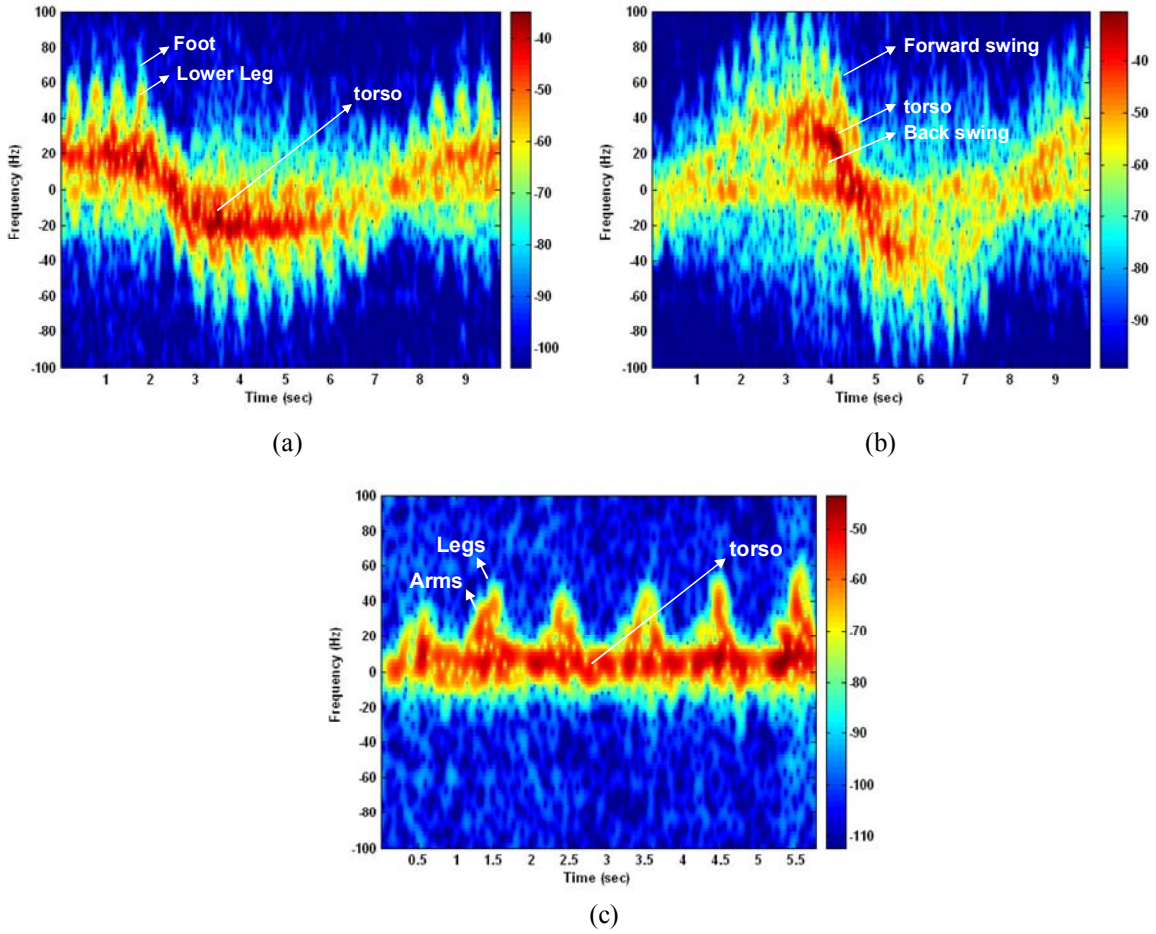

Fig. 2. Doppler spectrograms of measured data at 2.4GHz obtained from (a) walking (b) running and (c) crawling motions.

IV. Comparison against Measurement Results

Next, the three animation motions are replicated in the laboratory by a human subject and measurement data are collected using a Doppler radar testbed. The testbed consists of an RF transmitter operating at 2.4GHz connected to a horn antenna. The receiver system consists of a microstrip antenna connected to a dual quadrature integrated receiver (Analog Devices AD8347). The received signal is amplified, downconverted and digitized. The sampling frequency of the A/D converter is 500Hz. First, we measure the Doppler returns from regular walking motion. The time-domain radar returns are processed using equation (4) and the resulting spectrogram is shown in Fig. 2a. It is observed that the spectrogram shows good correspondence to the spectrogram generated by the simulated walking pattern shown in Fig. 1b. The Doppler components from the torso and the lower legs and feet are easily discerned. Next the measurement is made for the running motion over a circular track and the resulting spectrogram is shown in. Fig.2b. Again, the result is similar to the spectrogram results obtained in Fig. 1d. Considerably high Doppler returns from the torso and the lower legs are observed. Also, the backswing of the legs and feet is more prominent. The DC line in the spectrogram comes from the residual clutter after the low-pass filter in the radar. Next, measurements are performed for the crawling motion of the human subject. The Doppler spectrogram is shown in Fig. 2c which shows good agreement with the simulated spectrogram shown in Fig. 1f. The spectrogram shows considerable deviations in the microDoppler features when compared to the spectrogram of a regular walking pattern in Fig. 2a. The Doppler from the body is very low due to the slow speed of the motion. Also, the microDoppler features of the legs have noticeably reduced and are comparable to the microDopplers from the arms. However, the two microDoppler features can be distinguished at some time instants, since the microDopplers of the arms slightly precede the microDopplers from the legs.

V. Analysis of Additional Simulation Data

Some additional simulation data are generated and analyzed using the same methodology discussed earlier. Fig. 3 shows the simulated Doppler spectrogram from a one-minute duration

Authorized licensed use limited to: Indraprastha Institute of Information Technology. Downloaded on July 20,2021 at 20:40:47 UTC from IEEE Xplore. Restrictions apply.

BVH file. The specific time intervals from different motions such as accelerated walking, running and

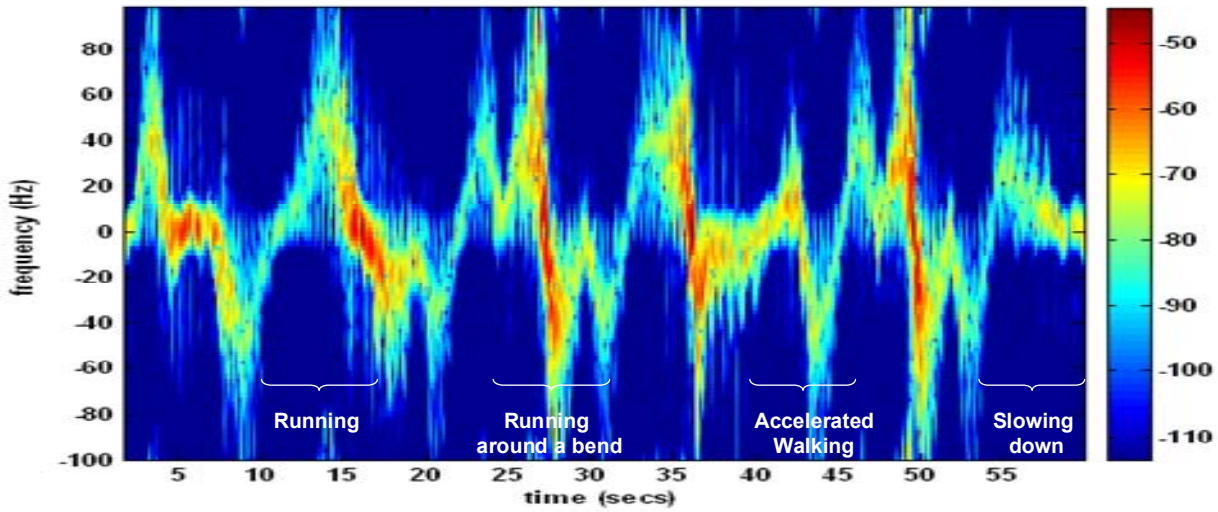

Fig. 3. Simulated Doppler signatures of human motions over a one-minute duration.

slowing down to a halt are marked in the spectrogram. Such data may be analyzed to study motion patterns for use in human activity monitoring over long durations.

The simulation model of the Doppler returns of complex human motions is also useful for performing feature-by-feature analysis of the microDoppler phenomena. Here, we repeat the simulation of the walking motion at 12 GHz and a 600Hz sampling frequency. The resulting spectrogram is shown in Fig. 4. Only a short span (3 seconds) of the spectrogram is shown in the figure. It is observed that due to the higher Doppler sensitivity at 12 GHz, it is possible to discern distinct microDoppler tracks of the different body parts such as the torso, lower arms, lower legs and feet. This spectrogram contrasts with the result at 2.4 GHz shown in Fig. 1b. The high frequency Doppler radar is thus useful for performing detailed analysis of the human gait. On the other hand, RF signal propagation through walls and obstructions favors the use of a lower operating frequency. Hence if the propagation effect is properly taken into account in the electromagnetic modeling, such tradeoffs can be studied and optimized in detail.

The Doppler spectrogram of the human motion is also dependent on the orientation of the mover with respect to the radar. To illustrate this effect, we next perform the simulation of the walking motion for a different position of the radar sensor at (0, 1, 5) m as shown in Fig. 4a. The resulting Doppler spectrogram is shown in Fig 4b. It is observed that the microDoppler returns are much lower in this case due to the low radial components of the velocity vectors. Thus, the effect of transceiver location on the microDoppler signature can be studied. The exploitation of multi-view information through a network of spatially diverse Doppler sensors can also be tested without having to first build such a system [9].

VI. Conclusion

A Doppler radar simulator of complex human motions is implemented using virtual reality animation data. The resulting spectrograms are compared against measured data obtained from a Doppler radar testbed operated in the laboratory. Additional simulation data are generated to study the effect of frequency and viewing angle. The simulator will provide us with the capability to study detailed Doppler phenomenology and to generate training data for algorithm development

Acknowledgment

This work is supported by the National Science Foundation under grant CBET-0730924 and in part by a grant from the NSF Major Research Instrumentation Program. We thank Prof. Arikan from the University of Texas at Austin and Sony Computer Entertainment America for the BVH motion capture data. The ASF/AMC data used in this project was obtained from mocap.cs.cmu.edu

References

[1] J. L. Geisheimer, E. F. Greneker and W. S. Marshall, "High-resolution Doppler model of the human gait," SPIE Proc. Radar Sensor Tech. Data Vis., vol. 4744, pp. 8 – 18, July 2002.

[2] V. C. Chen and H. Ling, Time Frequency Transforms for Radar Imaging and Signal Analysis, Artech House, Boston, MA, 2002.

[3] P. van Dorp and F. C. A. Groen, "Human walking estimation with radar," IEE Proc. Radar Sonar Navigation, vol. 150, pp. 356 – 365, Oct. 2003.

[4] M. Otero, "Application of continuous wave radar for human gait recognition," SPIE Proc., Signal Processing, Sensor Fusion, and Target Recognition XIV, vol. 5809, pp. 538 – 548, May 2005.

[5] M. D. Anderson and R. L. Rogers, "Micro-Doppler analysis of multiple frequency continuous wave radar signatures," SPIE Proc., Radar Sensor Technology XI, Volume 6547, pp. 65470A, May 2007.

[6] James Avro, Graphic Gems II, Academic Press Inc, Ithaca, New York, 1991.

Authorized licensed use limited to: Indraprastha Institute of Information Technology. Downloaded on July 20,2021 at 20:40:47 UTC from IEEE Xplore. Restrictions apply.

[7] J. W. Crispin, Jr. and A. L. Maffett, "Radar cross-section estimation for simple shapes," Proc. IEEE, pp. 833 – 848, Aug. 1965.
[8] C. Gabriel, S. Gabriel and E. Corthout, "The dielectric properties of biological tissues. I. Literature Survey," Phys. Med. Biol., vol. 41, pp. 2231 – 2249, 1996.
[9] Y. Kim and H. Ling, "Tracking a moving target with multiple Doppler sensors using artificial neural network," International IEEE AP-S Symposium, Honolulu, HI, June 2007.

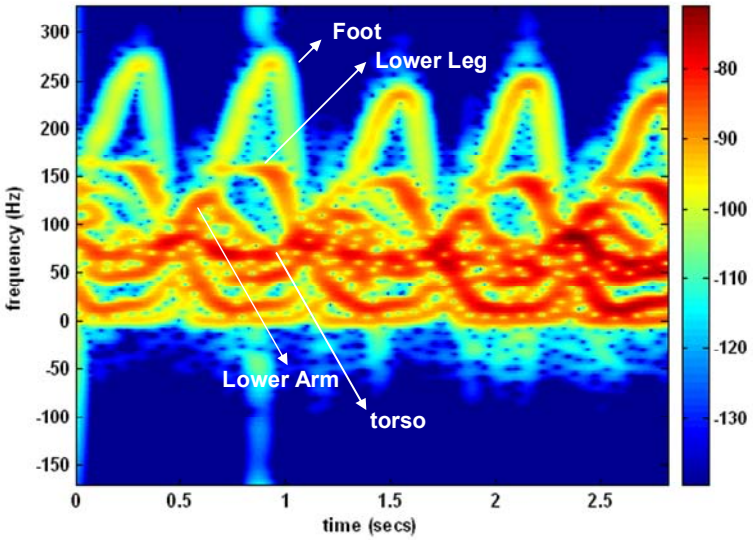

Fig. 4. Simulated Doppler spectrogram of walking motion at 12GHz

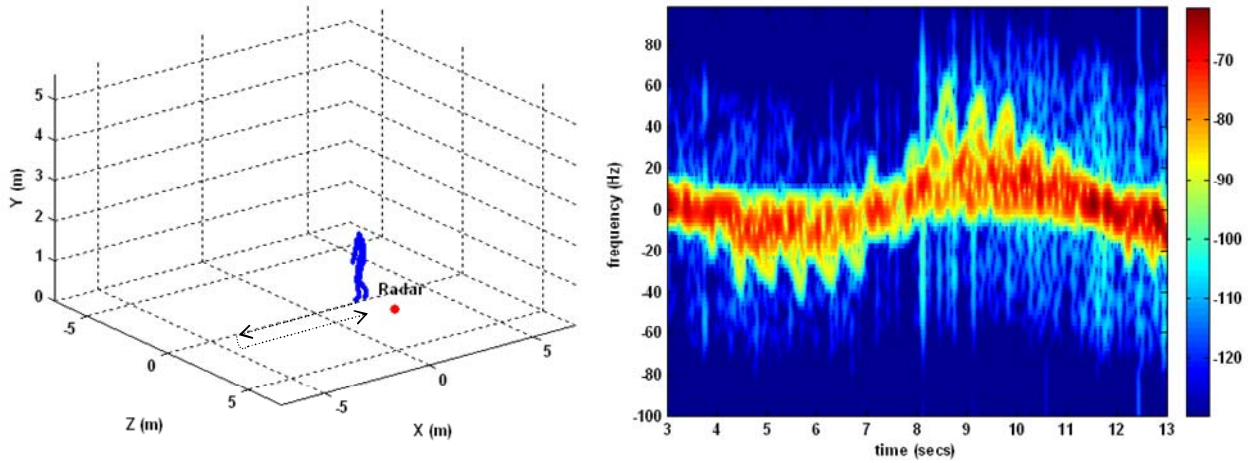

(a) (b)

Fig. 5. (a) Animation model of human walking motion across the radar's field of view. (b) Doppler spectrogram of walking motion at 2.4GHz carrier frequency

Authorized licensed use limited to: Indraprastha Institute of Information Technology. Downloaded on July 20,2021 at 20:40:47 UTC from IEEE Xplore. Restrictions apply.